Vol. 54: 85–93, 2012
doi: 10.3354/cr01109

CLIMATE RESEARCH
Clim Res

Published online August 22

Local effects of climate change over South Korea with a high-resolution climate scenario

Sanghun Lee, Deg-Hyo Bae*

Department of Civil and Environmental Engineering, Sejong University, Seoul 143-747, Korea

ABSTRACT: To evaluate the local effect of climate change over South Korea, a 5 km high-resolution climate scenario, based on general circulation model data to which a greenhouse gas scenario was applied, was created using SubBATS (a mosaic-type parameterization to account for subgrid-scale topography and land-use effects) from the regional climate model RegCM3. This high-resolution climate scenario shows that the simulated climatology is well reproduced both temporally and spatially. The results show an increase in annual temperature at 2 m over South Korea of approximately 4.6°C in the late 21st century. This increase is higher in winter and in September than at other times of year; the regional temperature increases, which are classified in 4 regions, display a variety of features. The temperature increase is significant in the regions with relatively low temperature. Yearly precipitation over South Korea is projected to show an overall increase of approximately 30% in the late 21st century. The precipitation increase is highest in August and varies by region. There is a close relationship between the precipitation increase and an increase in atmospheric water vapor. The rate of temperature increase grows with increasing altitude in all seasons. The increasing variation of precipitation is smaller with increasing altitude. Furthermore, the temperature and precipitation changes that accompany increasing altitude have a close relationship with the weakening of monsoons.

KEY WORDS: Regional climate change · Local effect · RegCM3 · Dynamic downscaling · South Korea

1. INTRODUCTION

Land cover and topography are among the major factors that influence local and regional climates (Pielke & Avissar 1990, Dickinson 1995). Complex topography and local land-surface features can modulate climate change signals by regulating land-atmosphere exchanges of heat, water, and momentum, thus modifying the structure of traveling synoptic systems, and triggering convection and mesoscale circulations (Giorgi & Mearns 1991, Giorgi & Avissar 1997, Pielke 2001, Feddema et al. 2005). Therefore, in climate simulations, it is important to account for the effects of complex topography and land cover. In regional downscaling, the complexity of the topography and land-surface structure are the most important factors. For this reason, different methods have been proposed to account for a subgrid-scale topography and land-use effects, such as multiple nesting (Christensen et al. 1998, Leung & Qian 2003, Im et al. 2006, 2010) and the parameterization of subgrid-scale processes (Giorgi & Avissar 1997). Other approaches provide representations of fine-scale land-surface processes. The most popular approach to representing the subgrid scale is the mosaic technique, in which a climate model grid box is divided into a set of subgrids. The subgrids can be based on homogeneous land-use surface categories (Avissar & Pielke 1989), homogeneous topography categories (Leung & Ghan 1995), or regular subgrid boxes, each characterized by its own land use type and elevation (Seth et al. 1994). Giorgi & Avissar (1997) discuss the

*Corresponding author. Email: dhbae@sejong.ac.kr

advantages and limitations of these different methods for representing land heterogeneity.

A higher resolution may be required to obtain useful information for input basin hydrology studies. Save4rivers is part of a new Korean project whose aim is to improve water management in South Korea as a coping strategy in response to climate change (www.4rivers.go.kr). South Korea is characterized by a complex topography in both its elevation and land-surface characteristics. The dynamical model, an upgraded version of the regional climate model RegCM3 (described by Pal et al. 2007), employs a much higher land-surface subgrid resolution of 5 km. The purpose of the present study is (1) to produce a high-resolution climate scenario for local effects of future climate change over South Korea, (2) validate the regional model's sensitivity via decadal simulation and (3) analyze the local and elevation effects of future climate change.

2. MODEL AND EXPERIMENT DESIGN

2.1. Regional climate model

In order to analyze regional climate change, a high-resolution climate scenario is required. Global climate scenario resolutions, however, are generally >100 km. To overcome this drawback, we used the regional climate model RegCM3 obtained from the International Centre for Theoretical Physics (ICTP) and described by Pal et al. (2007). It is an upgraded version of a model originally developed by Giorgi et al. (1993a,b) and later improved, as discussed by Giorgi & Mearns (1999). The physical parameterizations employed in the simulations include a radiative transfer package of the National Center for Atmospheric Research (NCAR) Community Climate Model, version 3 (Kiehl et al. 1996), the non-local boundary layer scheme of Holtslag et al. (1990), the mass-flux cumulus cloud scheme of Grell (1993), and the resolvable-scale cloud and precipitation scheme of Pal et al. (2000). The surface physics processes are described by the Biosphere-Atmosphere Transfer Scheme (BATS) land surface scheme (Dickinson et al. 1993), which is a land surface package designed to describe the role played by vegetation and interactive soil moisture in modifying the surface-atmosphere exchanges of momentum, energy, and water vapor.

The mosaic-type parameterization by Seth et al. (1994)—SubBATS—is implemented within RegCM3 as documented by Giorgi et al. (2003). In SubBATS, each grid cell of the dynamical model is divided into N regularly spaced subgrid cells of equal area, each with its own specification of topographical elevation, vegetation class, and soil type. In terms of input from the atmospheric model, BATS requires solar and infrared downward radiative fluxes, precipitation, near-surface air temperature, water vapor, wind speed, pressure, and density. After the calculations pertaining to land-surface processes are completed, BATS returns to the atmospheric model values for the albedo, surface upward infrared flux, momentum flux, sensible heat flux, and latent heat flux. Because the atmospheric model is run on a coarse grid and BATS on a fine subgrid, the atmospheric input to BATS needs to be disaggregated from the coarse grid to the subgrid. Based on Giorgi et al. (2003), the model grid to subgrid atmospheric input disaggregation is only based on the coarse and fine-grid topographical information, in our standard setup, which is the same as in Giorgi et al. (2003). Specific formulas are described in Giorgi et al. (2003). Similarly, the fine-scale SubBATS information needs to be reaggregated on the RegCM3 grid scale. The high-resolution projections can produce reliable estimations using SubBATS from RegCM3, even though South Korea is characterized by complex elevation and land-surface features. As for dynamic downscaling using RegCM3, a 1-way doubled-nested system was found to be effective (Im et al. 2006, 2010).

2.2. Simulation design

The regional climate model can be run under initial and lateral boundary conditions drawn from either global analysis data or from general circulation model (GCM) output. For the present study, the 1-way doubled-nested system of RegCM3 was used (Im et al. 2006, 2010). The mother domain covers the eastern regions of Asia (including the Korean peninsula) with a grid spacing of 60 km, whereas the nested domain focuses on South Korea with a grid spacing of 20 km. The subgrid cells in the 5 km grid spacing cover the same period as the nested domain. In all the experiments, the initial and time-dependent lateral boundary conditions were interpolated to an interval of 3 h. The simulation was driven at the lateral boundary by the atmosphere-ocean GCM called ECHO-G (Max Planck Institute for Meteorology, Models and Data Group). ECHO-G is a coupled model composed of an atmospheric part (ECHAM4) and an oceanic part (HOPE-G). This model is used for climate simulation, based on the future greenhouse gas emission scenario of the IPCC Special Report on

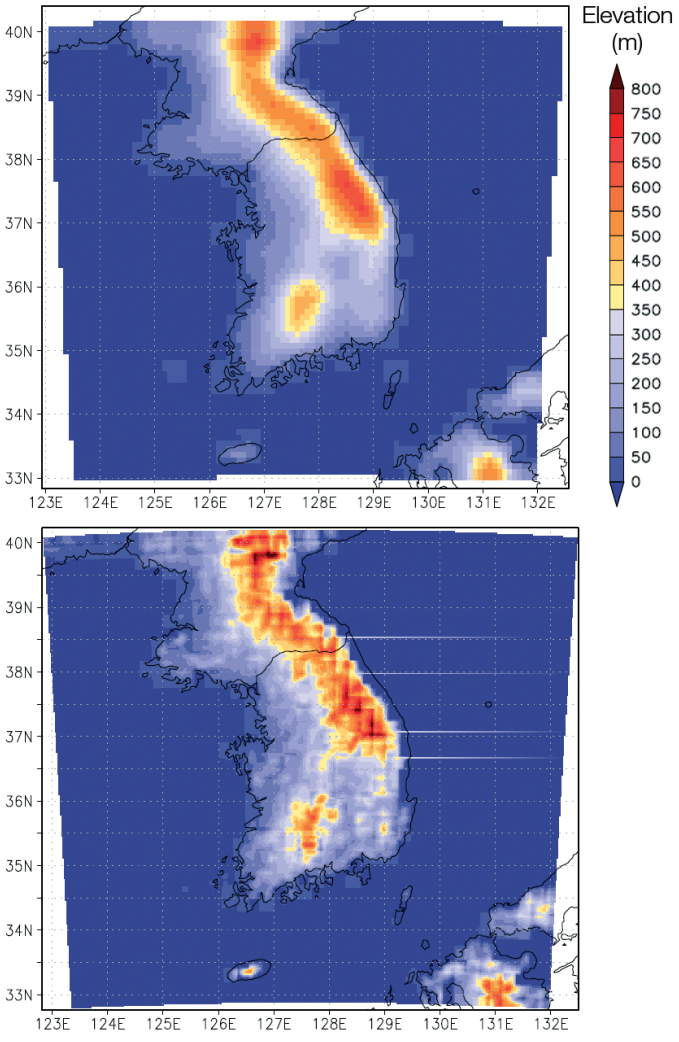

Fig. 1. Model domain and topography used for the (a) nested model grid (20 km grid spacing) and (b) subgrid (5 km grid spacing)

Emissions Scenarios (SRES) A2 scenario (METRI 2004). The output of ECHO-G has a horizontal resolution of 350 km at the tropics. The simulation continuously spans the 130 yr period from January 1, 1971 through December 31, 2100. Fig. 1 shows the model domain and topography used for the nested model grid (20 km) and the subgrid (5 km). The domain encompasses the Korean peninsula region. The nested grid cell size is 20 × 20 km on a Lambert conformal projection and the subgrid cell size is 5 × 5 km. Therefore, each nested grid cell is divided into 16 subgrid cells. The topographical information used to obtain the 2 grids was taken from a 2′ resolution global dataset produced by the US Geological Survey. Additionally, we used the 2′ resolution global land cover characterization datasets.

Our study focuses on temperature and precipitation. Fifty-seven stations were selected in order to examine their spatial distribution, and 18 major stations were selected to investigate the local effects of future climate change (Fig. 2). To analyze the local effects of future climate change, we compared the reference period (1971 to 2000) with the predicted future period (2071 to 2100) for temperature and precipitation using the results obtained from the 18 major stations. To assess the local effects over South Korea, we separated the South Korea mainland into 4 regions based on the results of Lee & Yamakawa (2006; see also Mun & Kim 1980, and Jeon et al. 1994): northwest, southwest, east, and south. As a result, the south and southwest regions were combined because the southwest region has no significant regional difference compared to other regions, while the inland region is included instead in order to investigate the differences between the coastal and inland regions (Fig. 3). To examine the effect of elevation, we selected the east-west cross-section at 37.2° N, with a transition from low terrain in the west to high in the east. Also, we selected an elevation range of 200 to 800 m in intervals of 100 m. The grid mean values were used for each elevation. Furthermore, in order to address changes in temperature and precipitation, we investigated the atmospheric water vapor and wind fields. The 57 observational datasets of the Korea Meteorological administration (KMA) were also used to evaluate the simulations. Also, temperature values from the Japanese 25 yr Reanalysis Project (JRA25) (1.25° × 1.25°) from Janu-

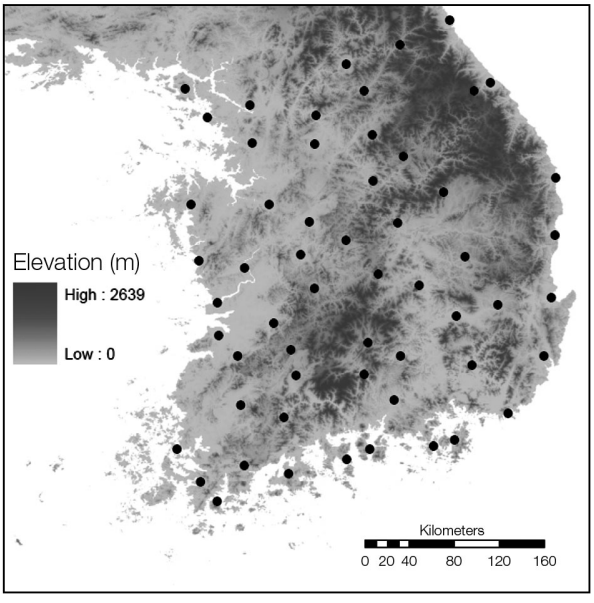

Fig. 2. Locations of 57 observational stations (●)

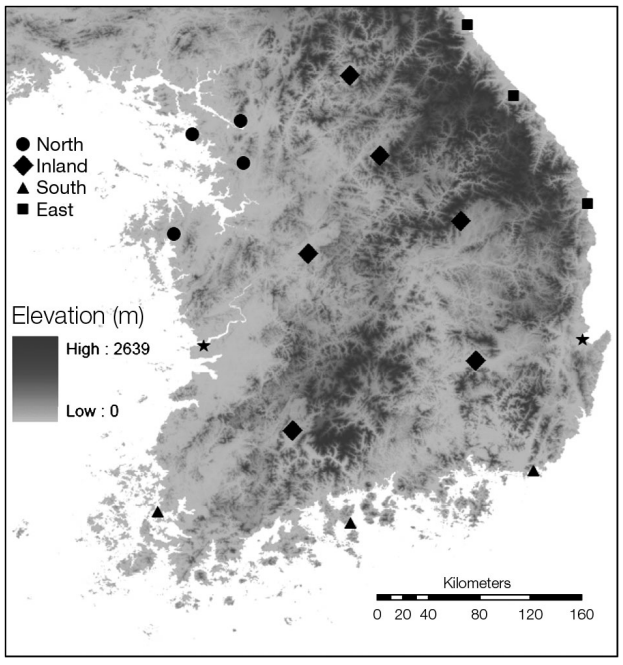

Fig. 3. Eighteen major stations and 4 regions over South Korea. (★) Not included in any region

ary 1979 to December 2000, and precipitation values of the Asian Precipitation-Highly-Resolved Observational Data Integration Towards Evaluation of the water resources project (APHRODITE) (0.25° × 0.25°) from January 1971 to December 2000 were used to evaluate the model's sensitivity.

3. RESULTS

3.1. Model sensitivity

In our sensitivity test, we focused mainly on the validation of the 5 km subgrid output. According to the model simulation results, the 5 km output indicates Korea's terrain better than the 20 km output (Fig. 1).

Fig. 4 shows the spatial distribution of the 30 yr average near-surface temperature and precipitation data for both the 5 km subgrid and from observations. Overall, the model results for temperature agree well with the observations. The correlation coefficients for spatial distribution were 0.93 (temperature) and 0.71 (precipitation) (the coefficient is significant at a 99% confidence level). The topographically induced spatial temperature distribution is well captured while the model result tends toward a cold bias. The model results of precipitation capture the topographically increased signature of the precipitation, but tend to underestimate it overall.

The model-output temperature values are similar to those in the reanalysis data. The highest correlation is between the JRA25 and the 5 km model output. The correlation coefficient is 0.98 between the 5 km output and JRA25 (the coefficient is significant at a 99% confidence level). The correlation coefficient is almost the same between JRA25 and the 60 and 20 km model outputs (Table 1), with the bias being <3°C on the 5 km subgrid. The correlation coefficient for temperature between the observation and the model output is similar to that of the reanalysis. Fig. 5 shows a time series (1981 to 1990) of the monthly precipitation data obtained from both the reanalysis data and the model outputs. The 5 km subgrid output of precipitation reproduces the results of APHRODITE well. The 5 km subgrid output reproduced the results of APHRODITE well, with an overall correlation coefficient of 0.56 (the coefficient is significant at a 99% confidence level). The correlation coefficient for the GCM output was barely 0.21. The precipitation model output showed good performance with increasing resolution (Table 1), with biases of <30% on the 5 km subgrid. The correlation coefficient for precipitation between the observation and the model output is almost similar to that obtained by the reanalysis. Also, the time-series correlation coefficients between the 5 km model output and the reanalysis data for the mean annual cycle were 0.93 for temperature and 0.61 for precipitation (the coefficient is significant at a 99% confidence level). Furthermore, improvement in performance with increasing resolution was more clearly shown in the model biases than in the correlation coefficients (Table 1). Although there is practically no difference in the correlation coefficient between 20 and 5 km, the difference in bias was >6% between the 20 and 5 km model outputs.

3.2. Future climate

Fig. 6 shows the monthly projected temperature change in the northwestern, eastern, southern, and inland regions of South Korea. The projections show an increase in the annual temperature means of approximately 4.6°C. The temperature increase is higher in the winter, and particularly in September, than it is in the other months. In the northern part of South Korea (between the northwestern and eastern regions), the increase in temperature differs from the western and eastern regions. From May to August, the temperature increase is greater in the eastern region than in the northwestern region, but the

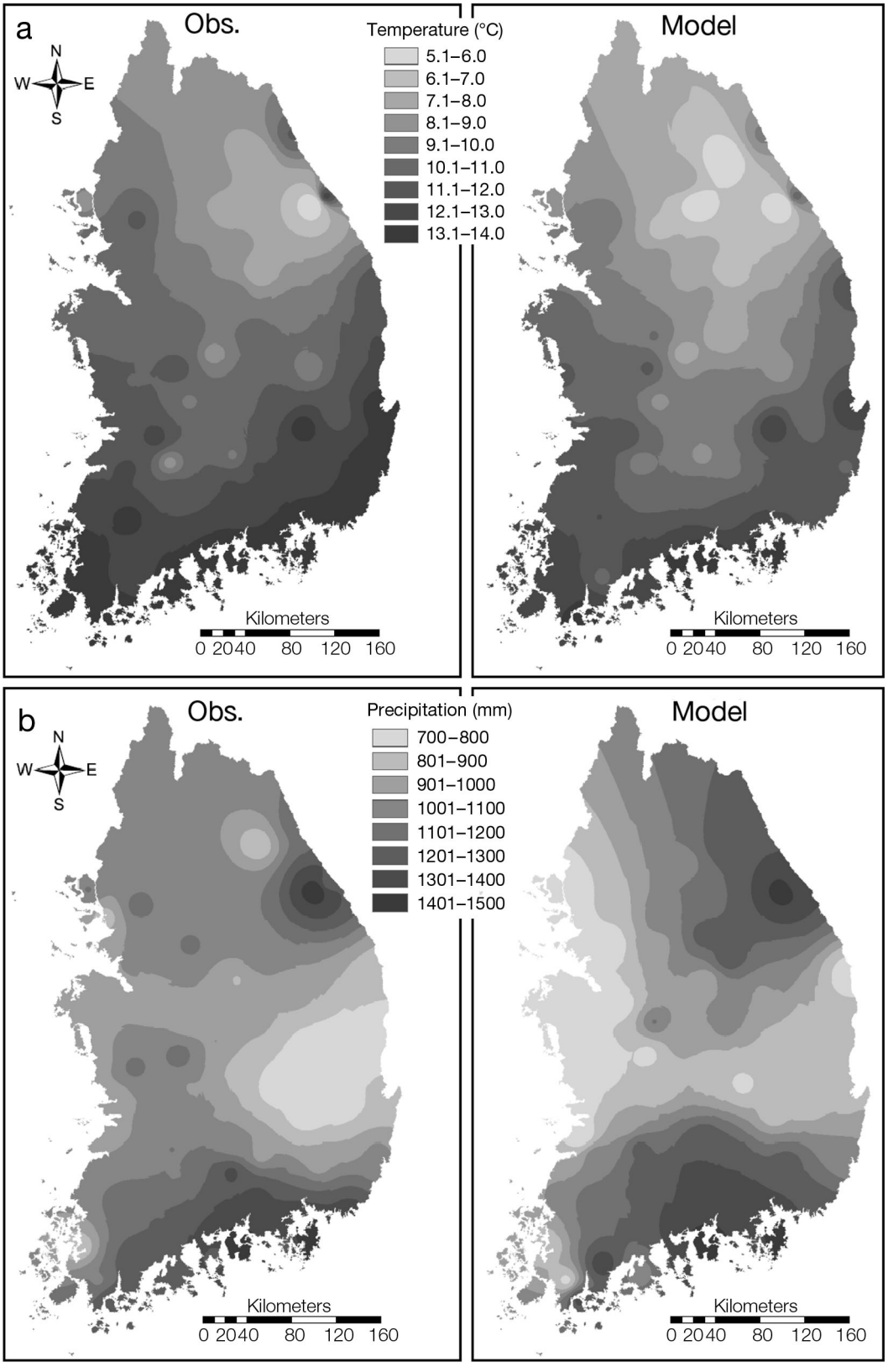

Fig. 4. Spatial distributions of observed and modeled 30 yr average (a) 2 m temperature and (b) precipitation, based on data from the 57 observational stations and the 5 km subgrid

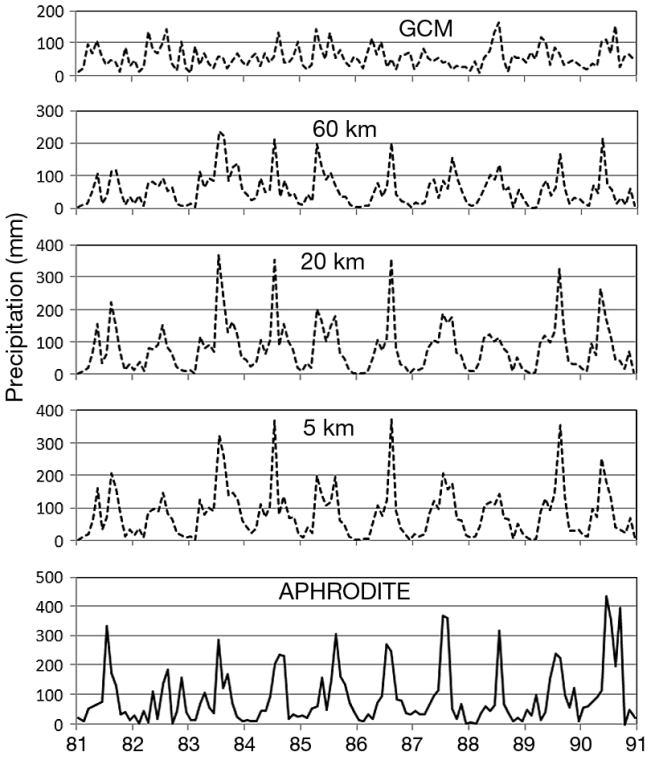

Fig. 5. Monthly change (January, 1981–1990) in reanalysis data and model outputs for precipitation drawn from mean values of data from 18 major stations

months in the rest of the year show an opposite trend. The temperatures in the northwestern and inland regions are similar. The temperature increase over the northwestern region from May to August is lower than that in the southern region, but again, the rest of the months show the opposite feature. Thus, the model predictions of future temperature over South Korea show an increase in temperature, throughout almost the entire year, with regional differences.

Fig. 7 shows the monthly projected precipitation changes in the northwestern, eastern, southern, and inland regions. The projections show an overall increase of approximately 30% in the annual precipitation over South Korea. This increase is highest in August. In the northern part of South Korea, the annual precipitation in the western region is approximately 170 mm greater than that in the eastern region. In most months, the northwestern region has a higher precipitation increase than the eastern region. The precipitation increase is small from October to April,

Table 1. Time-series correlation coefficients and biases of temperature (1979–2000) and precipitation (1971–2000) from mean values drawn from 18 major stations

	Temperature			Precipitation		
	Reanalysis	Obs.	Bias (°C)	Reanalysis	Obs.	Bias (%)
GCM	0.97	0.97	3.1	0.21	0.18	45.8
60 km	0.97	0.97	3.1	0.36	0.33	45.3
20 km	0.97	0.97	3.1	0.54	0.53	34.6
5 km	0.98	0.98	2.9	0.56	0.55	28.1

and in some months there is a decrease in the eastern and southern regions. The precipitation increase is higher from May to September, and in the north, from May to July it is higher than the eastern and southern regions. Apart from the period March to May, the northwestern and inland regions have almost the same feature. Thus, the model predictions of future precipitation over South Korea show an increase in precipitation, throughout almost the entire year, with regional differences.

Fig. 8 shows the monthly projected atmospheric water vapor change in the northwestern, eastern, southern, and inland regions. The projections show an approximately 40% overall increase in the annual atmospheric water vapor. The atmospheric water vapor increase in the winter and in September was higher than at other times of the year, and there are clear regional differences in the winter and in September. The monthly water vapor increase was similar to the precipitation increase in most months.

We also examined the effects of climate change at different elevations. Fig. 9 shows changes in temperature and precipitation at each elevation. The temperature change over South Korea increases with

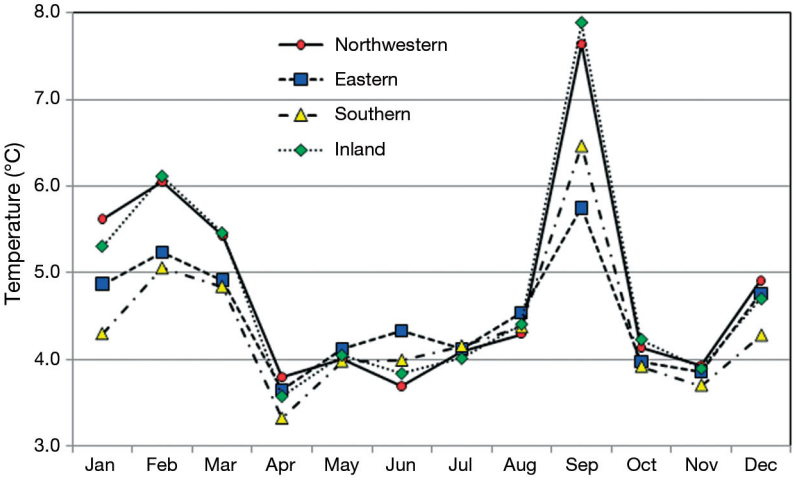

Fig. 6. Monthly future temperature change for the projected future period (2071–2100) minus the reference period (1971–2000) in the 4 regions

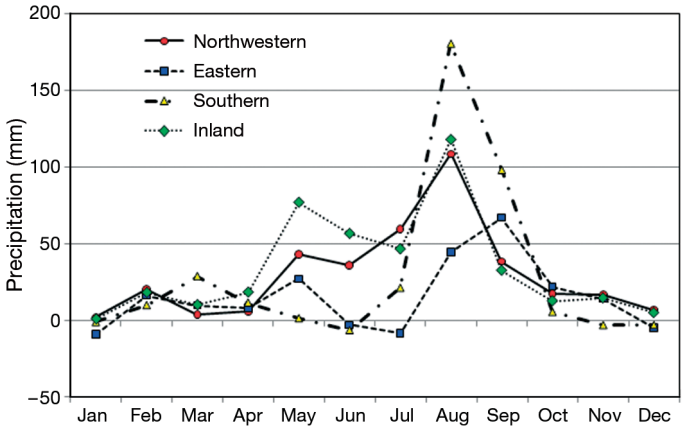

Fig. 7. Monthly future precipitation change for the projected future period (2071–2100) minus the reference period (1971–2000) in the 4 regions

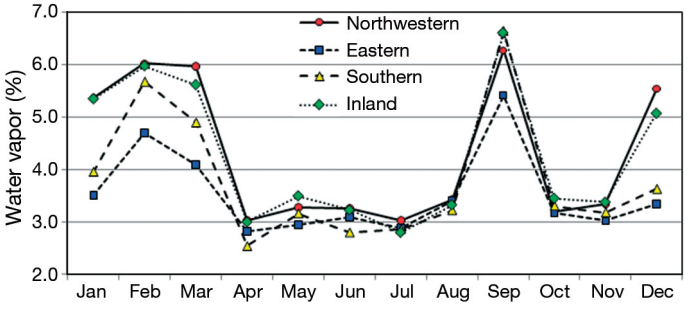

Fig. 8. Monthly future atmospheric water vapor change for the projected future period (2071–2100) minus the reference period (1971–2000) in the 4 regions

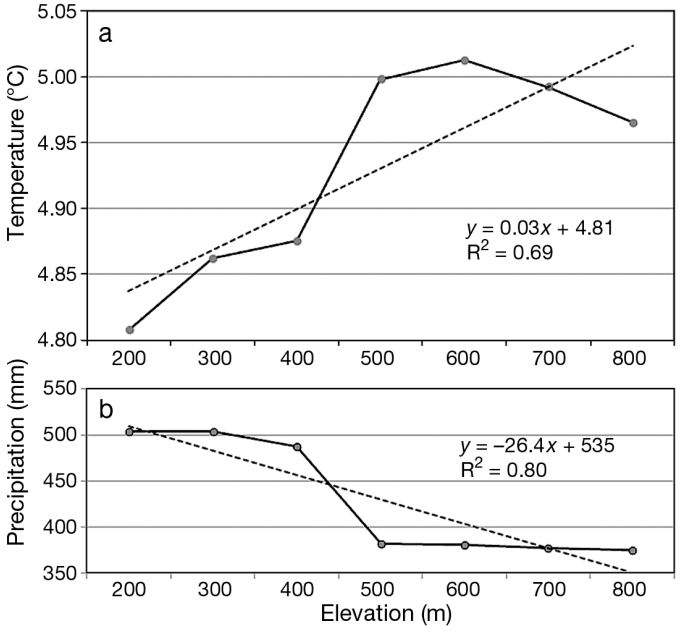

Fig. 9. (a) Temperature and (b) precipitation change for the projected future period (2071–2100) minus the reference period (1971–2000) for each elevation

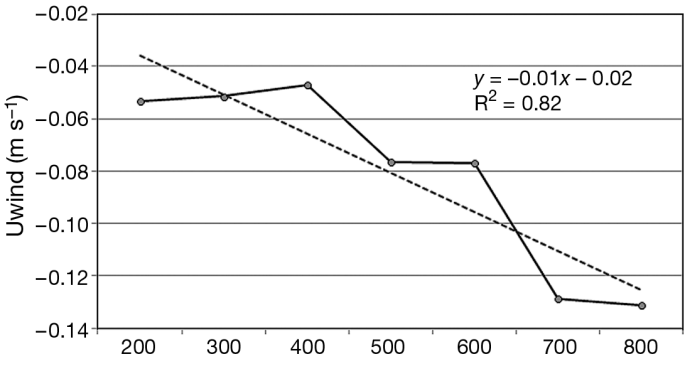

Fig. 10. Uwind change for the projected future period (2071–2100) minus the reference period (1971–2000) with variations for each elevation

increasing altitude in all seasons (R^2 = 0.69). This temperature increase is statistically significant from 200 to 600 m, and the increasing trend continues through all seasons. In contrast, the precipitation change in South Korea at each elevation decreases with increasing altitude in all seasons (R^2 = 0.80). Moreover, the precipitation change at each elevation shows an increasing trend in all seasons.

The relationship between the effects on elevation and wind speed was also investigated. Fig. 10 shows the Uwind (zonal wind) change at each elevation, which indicates a weakening trend with increasing altitude for all seasons.

4. DISCUSSION

To evaluate the local effects of future climate change over South Korea, we produced a 5 km high-resolution climate scenario using SubBATS from the RegCM3 model. The effectiveness of the high-resolution scenario with SubBATS was validated by Im et al. (2010). The high-resolution climate scenario shows that the model reproduces the climatology of the model domain well. Both the spatial and temporal patterns of temperature and precipitation over South Korea are well simulated. In particular, the topographic forcing on South Korea for temperature and precipitation are well captured. The simulation of precipitation is underestimated. A possible reason is that typhoons and rain fronts in the summer season are not well simulated by the low-resolution GCM. Despite a 30% bias in model precipitation, we still wanted to conduct the study, because the temporal and spatial variability is fairly well simulated. Also, the correlation between observed and simulated precipitation increases with finer resolution. This result means that the correlation increased because the terrain effect was clearly shown at a higher resolution.

According to the IPCC SRES A1B scenario, climate change in the late 21st century (2071 to 2100), as compared to that in the late 20th century (1971 to 2000), will increase by 4°C along the Korean peninsula, and by 3.8°C in South Korea (NIMR 2009). In the A2 scenario, stronger warming is seen, compared to the A1B scenario (Boo et al. 2006, NIMR 2008). The present study projects that the annual temperature over South Korea will increase by approximately 4.6°C. The finding that the temperature increase in winter season will be greater than in other seasons has been reported in several studies (IPCC 2007, NIMR 2008). Furthermore, the temperature increase in September is greater than it is in the other months, because the duration of the summer season is expected to lengthen owing to climate change (NIMR 2008).

Temperature changes in the northwestern region differ from those in the warmer eastern region, owing to a föhn effect produced in the Taebeck mountain range, which is centered between the 2 regions. Although the eastern region is at a higher elevation than the southern region, the temperatures in these 2 regions are similar because of the warming effects of the East Korean warm current (Kim & Yoon 1996) or that of the Tsushima warm current (Hase et al. 1999) in the eastern region.

The precipitation in the late 21st century as compared with the 20th century is projected to increase by 17% in all parts of Korea, as is suggested in scenario A1B, and in South Korea, it is expected to increase by 13% (NIMR 2008). Also, the precipitation increase in Korea will be highest in September and August. Hong et al. (2010) showed that the accumulated precipitation in the summer of the 2050s would be twice as much as that produced in the current climate. All previous studies have considered that the precipitation increase in South Korea is caused by increased humidity (NIMR 2008, Hong et al. 2010). The precipitation results in the present study are similar to those of previous studies, in that they show an overall increase in precipitation. Moreover, the atmospheric water vapor change is similar to the precipitation change. This means that the precipitation increase is due to the increase in atmospheric water vapor, which is in turn caused by the temperature increase. In particular, we obtained detailed estimates of the precipitation increase in the various regions of South Korea.

The effect of elevation on temperature is significant, with temperature increasing with altitude in all seasons. This result indicates that regions with low temperatures and high altitudes are particularly susceptible to global warming. In particular, the temperature increase is affected by a weakened monsoon.

South Korea is strongly affected by monsoons in winter and summer; therefore, precipitation is high in the high-altitude regions because of the topographic effect of strong monsoons. The present study shows that the precipitation increase becomes smaller with increasing altitude in all seasons, and thus the effect of elevation is weakened owing to weakened monsoons. The temperature and precipitation change may be closely related to the weakened monsoons that are an expected result of global warming.

5. SUMMARY

In this study, to evaluate the local effects of future climate change, we produced a 5 km high-resolution climate scenario using SubBATS of the RegCM3 model. The high-resolution climate scenario showed that the model reproduces the climatology of the simulated region and both the spatial and temporal patterns of temperature and precipitation over South Korea with a fair degree of accuracy.

An increase in the annual temperature mean over South Korea of approximately 4.6°C was projected for the late 21st century. The temperature increase during the winter and in September was greater than in other months. In particular, the regional temperature changes differed in the northwestern, eastern, southern, and inland regions. The precipitation change over South Korea showed an approximate 30% overall increase in the late 21st century. The precipitation increase reached a peak in August. There were different precipitation increases in the four study regions of the northwestern, eastern, southern, and inland regions. Moreover, the precipitation increase was caused by increased atmospheric water vapor.

The effects of elevation on temperature over South Korea were also examined, and the results showed that the rate of heating increases with altitude in all seasons. The temperature increase was particularly significant from 200 to 600 m altitude. This was in contrast to the precipitation change with elevation, which indicates a decrease in precipitation with increasing altitude for all seasons. There was also a relationship between the elevation effect and the weakening of monsoons.

The local effects analyzed in this study will be useful in establishing future climate adaptation measure over South Korea. However, this study used the A2 scenario of IPCC AR4 only. We will be able to obtain more useful results using various climate scenarios or the Representative Concentration Pathway of IPCC AR5.

Acknowledgements. This study was supported by the Construction Technology Innovation Program (09-Tech-Innovation -C01) through the Climate Change Assessment and Projection for Hydrology (CCAPH-K) under the Korea Institute of Construction & Transportation Technology Evaluation and Planning (KICTEP) of the Ministry of Land, Transport and Maritime Affairs (MLTM). Also, this work was supported by the National Research Foundation of Korea (NRF) grant funded by the Korean government (MEST) (No. 2011-0030839). We also gratefully acknowledge the comments and suggestions of E. S. Im and Jinho Shin of the Korean Meteorological Administration.

LITERATURE CITED

Avissar R, Pielke RA (1989) A parameterization of heterogeneous land surfaces for atmospheric numerical models and its impact on regional meteorology. Mon Weather Rev 117:2113–2136

Boo KO, Kwon WT, Baek HJ (2006) Changes of extreme events of temperature and precipitation over Korea using regional projection of future climate change. Geophys Res Lett 33:L01701 doi:10.1029/2005GL023378

Christensen OB, Christensen JH, Machenauer B, Botzet M (1998) Very high-resolution regional climate simulations over Scandinavia—present climate. J Clim 11:3204–3229

Dickinson RE (1995) Land-atmosphere interaction. Rev Geophys 33:917–922

Dickinson RE, Henderson-Sellers A, Kennedy PJ (1993) Biosphere-Atmosphere Transfer Scheme (BATS) version 1E as coupled to the NCAR Community Climate Model. NCAR Tech Note NCAR/TN-387+STR. National Center for Atmospheric Research, Boulder, CO

Feddema JJ, Oleson KW, Bonan GB, Mearns LO, Buja LE, Meehl GA, Washington WM (2005) The importance of land-cover change in simulating future climates. Science 310:1674–1678

Giorgi F, Avissar R (1997) The representation of heterogeneity effects in earth system modeling: experience from land surface modeling. Rev Geophys 35:413–438

Giorgi F, Mearns LO (1991) Approaches to the simulation of regional climate change: a review. Rev Geophys 29: 191–216

Giorgi F, Mearns LO (1999) Introduction to special section: regional climate modeling revisited. J Geophys Res Atmos 104:6335–6352

Giorgi F, Marinucci MR, Bates GT (1993a) Development of a second-generation regional climate model (RegCM2). 1. Boundary-layer and radiative transfer processes. Mon Weather Rev 121:2794–2813

Giorgi F, Marinucci MR, Bates GT, De Canio G (1993b) Development of a second-generation regional climate model (RegCM2). 2. Convective processes and assimilation of lateral boundary conditions. Mon Weather Rev 121:2814–2832

Giorgi F, Francisco R, Pal J (2003) Effects of a subgrid-scale topography and land use scheme on the simulation of surface climate and hydrology. 1. Effects of temperature and water vapor disaggregation. J Hydrometeorol 4: 317–333

Grell GA (1993) Prognostic evaluation of assumptions used by cumulus parameterizations. Mon Weather Rev 121: 764–787

Hase H, Yoon JH, Koterayama W (1999) The current stricture of the Tsushima Warm Current along the Japanese coast. J Oceanogr 55:217–235

Holtslag AAM, de Bruijn EIF, Pan FL (1990) A high resolution air mass transformation model for short-range weather forecasting. Mon Weather Rev 118:1561–1575

Hong SY, Moon NK, Lim KSS, Kim JW (2010) Future climate change scenarios over Korea using a multi-nested downscaling system: a pilot study. Asia-Pac J Atmos Sci 46: 425–435

Im ES, Park EH, Kwon WT, Giorgi F (2006) Present climate simulation over Korea with a regional climate model using a one-way double-nested system. Theor Appl Climatol 86:187–200

Im ES, Coppola E, Giorgi F, Bi X (2010) Validation of a high-resolution regional climate model for the Alpine region and effects of a subgrid-scale topography and land use representation. J Clim 23:1854–1873

IPCC (2007) Core Writing Team, Pachauri RK, Reisinger A (eds) Climate change 2007: synthesis report. Contribution of Working Groups I, II and III to the Fourth Assessment Report of the Intergovernmental Panel on Climate Change. IPCC, Geneva

Jeon J, Lee D, Lee H (1994) A study on the heavy snowfalls occurred in South Korea. J Korean Meteorol Soc 30: 97–117 (in Korean)

Kiehl JT, Hack JJ, Bonan GB, Boville BA, Briegleb BP, Williamson DL, Rasch PJ (1996) Description of NCAR Community Climate Model (CCM3). NCAR Tech Note NCAR/TN-420+STR. National Center for Atmospheric Research, Boulder, CO

Kim CH, Yoon JH (1996) Modeling of the wind-driven circulation in the Japan Sea using a reduced gravity model. J Oceanogr 52:359–373

Lee S, Yamakawa S (2006) Wintertime climate classification and climatological features of South Korea. J Agric Meteorol 62:53–63

Leung LR, Ghan SJ (1995) A subgrid parameterization of orographic precipitation. Theor Appl Climatol 52:95–118

Leung LR, Qian Y (2003) The sensitivity of precipitation and snowpack simulations to model resolution via nesting in regions of complex terrain. J Hydrometeorol 4:1025–1043

METRI (METeorological Research Institute, Korea) (2004) Research on the development of regional climate change scenarios to prepare the national climate change. III. METRI, Seoul (in Korean)

Mun S, Kim S (1980) On the distribution of winter precipitation according to the passage of front and/or low in Korea. J Korean Meteorol Soc 16:1–13 (in Korean)

NIMR (National Institute of Meteorological Research) (2008) The application of regional climate change scenario for the national climate change (IV). NIMR, Seoul

NIMR (National Institute of Meteorological Research) (2009) Understanding of climate change II. NIMR, Seoul

Pal JS, Small EE, Eltahir EAB (2000) Simulation of regional-scale water and energy budgets: representation of subgrid cloud and precipitation processes within RegCM. J Geophys Res Atmos 105:29576–29594

Pal JS, Giorgi F, Bi X, Elguindi N and others (2007) Regional climate modeling for the developing world: the ICTP RegCM3 and RegCNET. Bull Am Meteorol Soc 88: 1395–1409

Pielke R (2001) Influence of the spatial distribution of vegetation and soils on the prediction of cumulus convective rainfall. Rev Geophys 39:151–177

Pielke R, Avissar R (1990) Influence of landscape structure on local and regional climate. Landscape Ecol 4:133–155

Seth A, Giorgi F, Dickinson RE (1994) Simulating fluxes from heterogeneous land surfaces: explicit subgrid method employing the biosphere-atmosphere transfer scheme (BATS). J Geophys Res Atmos 99:18651–18667

Editorial responsibility: Bryson Bates, Wembley, Australia

Submitted: July 26, 2011; Accepted: May 2, 2012
Proofs received from author(s): August 14, 2012